Initiation of Sodium Spikelets in Basal Dendrites of Neocortical Pyramidal Neurons

B.A. Milojkovic[1], J.P. Wuskell[2], L.M. Loew[2], S.D. Antic[3]

[1]Department of Neuroscience, Erasmus MC Dr. Molewaterplein 50, 3015 GE, Rotterdam, Netherlands
[2]Department of Cell Biology, UConn Health Center, 263 Farmington Ave., CT 06030, USA
[3]Department of Neuroscience, L-4000, UConn Health Center, 263 Farmington Ave., Farmington, CT 06030-3401, USA

Abstract. Cortical information processing relies critically on the processing of electrical signals in pyramidal neurons. Electrical transients mainly arise when excitatory synaptic inputs impinge upon distal dendritic regions. To study the dendritic aspect of synaptic integration one must record electrical signals in distal dendrites. Since thin dendritic branches, such as oblique and basal dendrites, do not support routine glass electrode measurements, we turned our effort towards voltage-sensitive dye recordings. Using the optical imaging approach we found and reported previously that basal dendrites of neocortical pyramidal neurons show an elaborate repertoire of electrical signals, including backpropagating action potentials and glutamate-evoked plateau potentials. Here we report a novel form of electrical signal, qualitatively and quantitatively different from backpropagating action potentials and dendritic plateau potentials. Strong glutamatergic stimulation of an individual basal dendrite is capable of triggering a fast spike, which precedes the dendritic plateau potential. The amplitude of the fast initial spikelet was actually smaller that the amplitude of the backpropagating action potential in the same dendritic segment. Therefore, the fast initial spike was dubbed "spikelet". Both the basal spikelet and plateau potential propagate decrementally towards the cell body, where they are reflected in the somatic whole-cell recordings. The low incidence of basal spikelets in the somatic intracellular recordings and the impact of basal spikelets on soma-axon action potential initiation are discussed.

Key words: Prefrontal cortex — Pyramidal neurons — Basal Dendrites — Synaptic integration — Dendritic — Spikes — Potentials — UP states

---

Correspondence to: S.D. Antic; email: antic@neuron.uchc.edu

Introduction

Pyramidal cells constitute the major cellular elements of the cerebral cortex, and it is widely believed that understanding their integrative properties holds a key to the mechanistic comprehension of cortical function. It is now well established that neuronal processes (dendrites) perform the critical initial stage of synaptic integration (Hausser, Spruston & Stuart, 2000; Magee, 2000; Larkum, Zhu & Sakmann, 2001; Poirazi, Brannon & Mel, 2003; London & Hausser, 2005). "Four factors – (1) Dendritic branching architecture, (2) Synaptic placement, (3) Passive, and (4) Active membrane properties – must be taken into account in assessing the nature of the integrative activity of dendrites" (Shepherd, 2004). Mammalian cortex is organized in six layers and distinct groups of synaptic inputs impinge on basal, oblique, and apical dendrites (Feldmeyer et al., 2002; Shipp & Zeki, 2002). Based on the first two factors ((1) Dendritic branching architecture; and (2) Synaptic placement), the three classes of pyramidal dendrites (basal, oblique, and apical) seem to have specialized functions (Larkum et al., 2001; Frick et al., 2003). Given the nonuniform spatial distribution of dendritic membrane conductances (Migliore & Shepherd, 2002; Trimmer & Rhodes, 2004) it is possible that basal, oblique, and apical dendrites also exhibit distinct passive and active membrane properties (factors 3 and 4). Putting this information together, it is very likely that different types of dendrites display different repertoires of electrical behavior.

Arguably the best way to investigate dendritic electrical properties is to record membrane potential directly from dendrites. The advent of dendritic patch electrode recordings produced detailed descriptions of dendritic passive (Stuart & Spruston, 1998) and active (Magee & Johnston, 1995; Bekkers, 2000) membrane properties (reviewed in (Gulledge, Kampa & Stuart, 2005)). However, these studies were carried out in one

particular dendritic type — the apical trunk. Due to their small size, basal and oblique dendrites do not support routine glass electrode recordings, and very little is known about their physiological properties.

To study thin dendrites, which are difficult to patch, one can use an alternative approach called "voltage imaging" (Djurisic et al., 2004). The advantages of optical recording of membrane potential changes over more traditional techniques were recognized long ago by Salzberg et al. (1977). Some of these include: (1) recording from inaccessible membranes, (2) preservation of mechanical integrity of the plasma membrane, and (3) the capability of recording simultaneously from very many points in an image. In the case of multi-site recordings from individual neurons and their processes, an intracellular, rather than extracellular, application of fluorescent voltage-sensitive dyes proved to be a more useful strategy (Davila et al., 1974; Grinvald et al., 1987; Antic & Zecevic, 1995).

In the present study we used styryl voltage-sensitive dyes designed for intracellular application (Loew et al., 1992), to monitor the spatial and temporal distribution of membrane potential along an individual basal branch, and, in some cases, along several dendritic branches simultaneously. We were particularly interested in the nature of dendritic electrical signals during the suprathreshold glutamatergic excitation that causes characteristic electrical signals in the cell body — sustained somatic depolarizations superimposed with burst firing of action potentials. Similar plateau depolarizations (UP states) are regularly recorded from somata of cortical pyramidal neurons in vivo (Steriade, Nunez & Amzica, 1993b; Lewis & O'Donnell, 2000). A combination of focal glutamate stimulation and voltage-sensitive dye measurements showed that basal dendrites possess a repertoire of electrical signals including backpropagating action potentials (Antic, 2003) and regenerative dendritic plateau potentials (Milojkovic, Radojicic & Antic, 2005). In the present study we report a novel, third type of electrical signal in basal dendrites of neocortical pyramidal neurons, a signal that is qualitatively and quantitatively different from backpropagating action potentials (BAPs) or dendritic plateau potentials (DPP). Here we present experimental evidence that basal dendrites have the ability to fire sodium spikelets in response to glutamatergic excitation.

Materials and Methods

Electrophysiology and Morphology

Sprague Dawley rats (P21 – 42) were anesthetized with halothane, decapitated, and the brain was removed with the head immersed in ice-cold, artificial cerebrospinal fluid (ACSF), according to an animal protocol approved by the Center for Laboratory Animal Care, University of Connecticut. Brain slices (300 μm) were cut from frontal lobes in the coronal plane. ACSF contained (in mM) 125 NaCl, 26 NaHCO$_3$, 10 glucose, 2.3 KCl, 1.26 KH$_2$PO$_4$, 2 CaCl$_2$ and 1 MgSO$_4$, pH 7.4. Tetrodotoxin (TTX, 1 μM) was purchased from Sigma. Whole-cell recordings were made at 30–33 °C from visually identified layer V pyramidal neurons on the medial and dorso-medial part of the slice. Intracellular solution contained (in mM) 135 K-gluconate, 2 MgCl$_2$, 3 Na$_2$-ATP, 10 Na$_2$-phosphocreatine, 0.3 Na$_2$-GTP and 10 HEPES (pH 7.3, adjusted with KOH). Electrical signals were amplified with Multiclamp 700A and digitized with two input boards: (1) Digidata Series 1322A (Axon Instruments) at 5 kHz, and (2) Neuroplex (RedShirtImaging) at 1 kHz sampling rate. Only cells with a membrane potential more hyperpolarized than −50 mV, and action potential amplitudes exceeding 80 mV (measured from the base line) were included in this study. To allow positioning of glutamate stimulation electrodes, neurons were filled through whole-cell recording pipettes containing either rhodamine-dextran 3000 (80–100 μM), Alexa Fluor 594 (60–100 μM) or voltage-sensitive dyes (see below), dissolved in standard K-gluconate based intracellular solution. After the experiment, fluorescence images were taken with a CCD camera (Dage IR-1000) on a Zeiss Axioskop 2FS. All fluorescent neurons ($n = 42$) had typical pyramidal morphology with thick apical dendrites projecting vertically towards the pia. The apical trunk bifurcation occurred high in layers III and II, giving rise to 2–3 apical tuft branches that run almost parallel to pia. Twenty-one out of 225 neurons, in which the stimulation pipette was positioned blindly ("sniffing for dendrites", see below), were filled with biocytin (0.5%) and processed with an avidin-based (Vectastain PK-6100 Standard) kit. All of the biocytin-filled cells exhibited typical layer V pyramidal morphology with tufted apical dendrites.

Optical Measurements

The voltage-sensitive dye JPW3028 was synthesized according to the palladium-catalyzed coupling pathway described by Hassner et al. (1984). The final step involved the alkylation of β-[2-(dimethylamino)-6-napthyl]-4-vinylpyridine with (2-bromoethyl) trimethylammonium bromide. The resultant dye (also called di-1-ANEPEQ) is a doubly positively charged analogue of the ANEPPS series (Loew et al., 1992) of lipophilic voltage-sensitive dyes that is still sufficiently water-soluble to be used for microinjection. The diethyl analog JPW 1114 (di-2-ANEPEQ) has recently become available from Molecular Probes Inc. (Eugene, OR). JPW 3028 and JPW 1114 were dissolved in intracellular solution (0.8–1.5 mM) and loaded into neurons through whole-cell pipettes (∼30 min). Loading pipettes were then pulled out (outside-out patch) and neurons were incubated at room temperature for 1–2 hours. Before optical recordings, neurons were transferred to a recording microscope equipped with a NeuroCCD camera (RedShirtImaging, LLC, Fairfield, CT) and repatched with dye-free electrodes. Six out of 34 neurons were not repatched (see Fig. 2). Dendrites were illuminated with a Xenon 250W short arc lamp (770 X W/T OptiQuip, Highland Mills, NY). Optical signals (excitation 520 ± 45 nm; dichroic 570 nm; emission > 610 nm) were recorded with 80 × 80 pixels at a 1 kHz frame rate, stored, and then temporally filtered (off-line) with digital Gaussian low-pass filter (300 Hz cut-off), and Butterworth high-pass (0.4 Hz), unless otherwise specified. To correct for photobleaching, the trace without stimulus was recorded at the end of each experiment and subtracted from the physiological recordings. We refer to a selected neuronal compartment as an ROI (region of interest), where membrane potential transients were measured either optically (voltage-sensitive dyes) or electrically (whole-cell). To improve the signal-to-noise ratio, multiple pixels (6 – 24) were selected inside the region of interest and spatially averaged (Fig. 1C).
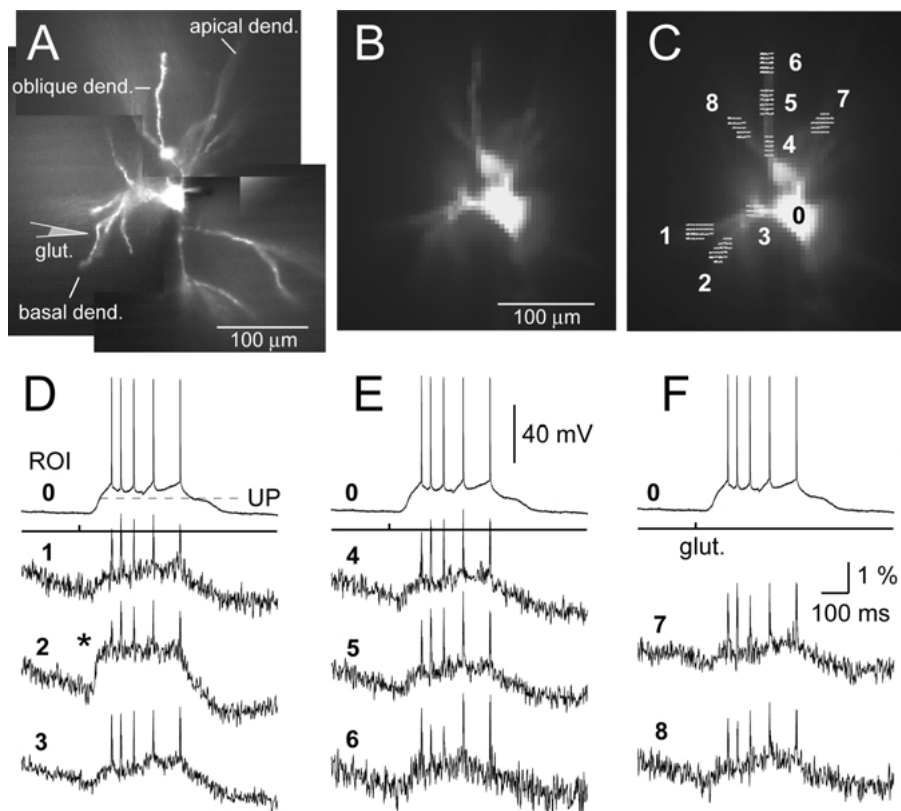
Fig. 1. AP backpropagation during suprathreshold excitatory stimulation. (*A*) High resolution composite photomicrograph of a prefrontal cortical pyramidal cell stained with JPW3028. The schematic drawing indicates the position of the glutamate-filled pipette on a basal dendrite 95 μm from the center of the soma. (*B*) One frame from a movie sequence taken with the data acquisition camera at 1 kHz sampling frequency (frame rate). (*C*) Same as in *B*, except 8 groups of pixels (1–8), from 8 regions of interest (ROIs), were selected across the dendritic tree. To identify pixels used for spatial averaging within the ROI, each selected pixel is shown with a tiny optical trace superimposed using the Neuroplex software. The sizes of ROIs selected for display in panels *D–F* were (in pixels): *1* = 22; *2* = 19; *3* = 12; *4* = 10; *5* = 18; *6* = 15; *7* = 19; and *8* = 16 pixels. The distances of ROIs from the center of the soma were (in μm): *1* = 100; *2* = 95; *3* = 45; *4* = 75; *5* = 115; *6* = 165; *7* = 95; and *8* = 110 μm. (*D*) The optical signal from the glutamate stimulation site (ROI *2*) is aligned with the optical signal from the proximal segment of the target dendrite (ROI *3*), non-target dendrite (ROI *1*) and electrical signal from the soma (ROI *0*). An asterisk indicates our failure to detect a fast transient on the rising phase of the dendritic glutamate-evoked plateau potential. (*E*) Optical signals from the oblique dendrite (ROIs *4–6*) are aligned with the somatic whole-cell recording. (*F*) Optical signals from two oblique branches are aligned with the somatic electrical trace. Note that all of the dendritic recordings show five action potentials having similar amplitude.

Glutamate Application

Sharp (40 ± 10 MΩ) pipettes were pulled from borosilicate glass capillary containing a filament (1.5 mm OD), and backfilled with 200 mM Na-glutamate (pH = 9). A programmable stimulator (Master-8) and stimulus isolation unit (IsoFlex; A.M.P.I., Jerusalem, Israel) were used iontophoretically to eject glutamate. A motorized micromanipulator (MP-285, Sutter Instruments) was used to drive the tips of glutamate pipettes diagonally ("fourth axis") into the slice tissue. In the "diagonal mode", both "*X*" and "*Z*" axis motors were engaged simultaneously. In experiments where glutamate iontophoresis pipettes were positioned blindly ("sniffing for dendrites"), two criteria were used to determine the adequate stimulation site. First, the tip of the stimulation pipette had to be more than 40 μm away from the cell body and more than 30 μm below the surface of the slice. Second, glutamate pulses of only 1.8 μA (5 ms duration) had to trigger >100 ms plateau depolarizations accompanied by at least one action potential (*see* Figs. 8 and 13). A glutamate pulse was considered "suprathresh-

old" if a single application produced >100 ms plateau depolarizations accompanied by at least one somatic action potential. It is worth mentioning that in numerous experiments (*n* > 80 neurons) the half-width of the glutamate-evoked sustained depolarization exceeded 400 ms, and was accompanied by more than 3 APs (Figs. 1, 2, 4, and 9–11). The great majority of glutamatergic stimulations (*n* > 150 neurons) were performed at distances larger than 80 μm from the center of the soma.

Synaptic Stimulation

In experiments where the release of endogenous glutamate was triggered by shocking presynaptic terminals, we used 7 MΩ patch pipettes filled with extracellular solution. After insuring that the tip of the stimulation electrode was positioned at less than 25 μm from the distal dendrite, electric shocks were delivered with fixed duration (100–200 μs), while current amplitude varied in the range of 10–90 μA. In 8 neurons, instead of one, we delivered a train of 3–6 pulses at 20 ms inter-stimulus interval (50 Hz).

DATA ANALYSIS

Optical and electrical measurements were analyzed using the software Neuroplex 5.03 (RedShirtImaging, LLC, Fairfield, CT) and Axoscope 8.1 (Axon Instruments). Graph plotting was done in Excel. Amplitudes of action potentials and spikelets in remote dendritic segments (optical signals) were measured from the base line and expressed as a fractional change in light intensity ($\delta F/F$). Intracellular voltage-sensitive dyes cannot be used to determine the absolute amplitude (in mV) of the electrical transients in distal dendritic segments (Antic, Major & Zecevic, 1999). However, voltage-sensitive dyes can be used to detect a relative amplitude change between signals obtained from the same dendritic segment in consecutive recording trials (Milojkovic et al., 2004). Since the concentration and partition of the voltage-sensitive dye in a given dendritic segment is unlikely to change significantly within a 2–3 min period, the sensitivity of voltage-sensitive dye measurements obtained from the same dendritic segment remains constant between successive recordings. Any difference in the optical signal amplitude between two consecutive sweeps is therefore due to the difference in the amplitude of the membrane potential transient. When comparing amplitudes of optical signals among consecutive sweeps we used the same set of selected pixels (ROI), and signals were spatially averaged to improve the signal-to-noise ratio. Examples of measurements performed from the same set of pixels in consecutive sweeps are displayed in Figs. 3, 6 and 7. In Figures 1–7 we adopted the following strategies: (1) all illustrated examples are temporally nonaveraged traces; (2) the size of the optical signals is expressed as $\delta F/F$ (%). (3) "glut." marks the timing of a single glutamate pulse (duration = 5 ms); and (4) Arabic numeral in front of a trace indicates an ROI.

Results

AP BACKPROPAGATION IN THIN DENDRITES RECEIVING STRONG GLUTAMATERGIC EXCITATION

In 34 neurons we monitored membrane potential transients along basal and near-oblique branches during glutamate-evoked UP–state-like depolarizations (Fig. 1). Glutamate pulses (duration = 5 ms) were delivered from glass pipettes positioned ~10 μm from the shaft of the selected basal dendrite, 30–80 μm under the surface of the brain slice (Fig. 1A). This type of stimulation is localized to an area with a radius smaller than 25 μm (Milojkovic et al., 2005). APs propagated strongly into the most distal tips of thin dendrites that were not exposed to glutamate (backpropagation). AP-associated optical signals were recorded in both basal (ROI 1) and near-oblique branches (ROIs 6 and 8). With the present level of signal-to-noise ratio, our method did not detect the frequency-dependent attenuation of action potential signals, which was previously described in apical dendrites of hippocampal (Spruston et al., 1995) and neocortical (Stuart, Schiller & Sakmann, 1997; Larkum et al., 2001) pyramidal cells. In the middle segments of the target dendrite (basal dendrite exposed to a glutamate pulse) the backpropagating APs were riding on top of the glutamate-evoked
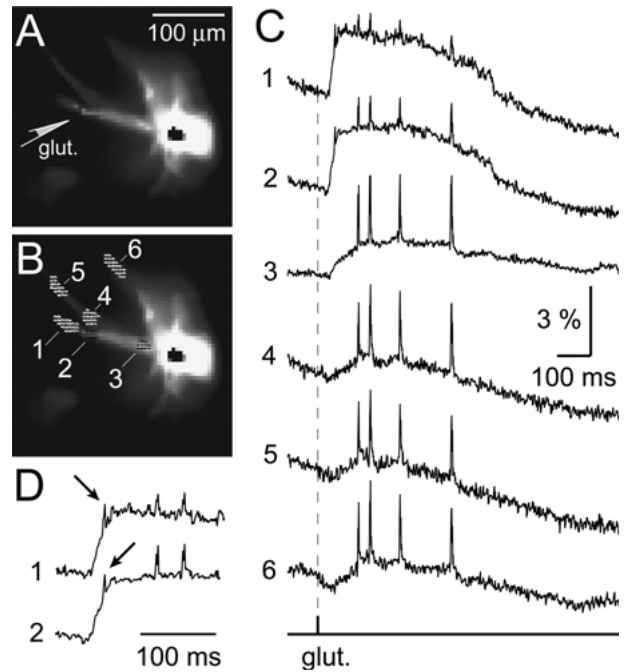

Fig. 2. Fast spikelet at the beginning of the dendritic plateau potential. (A) One frame selected from the sequence of frames (movie) capturing the glutamate-evoked plateau potential in the basal dendritic tree. The dark region in the center of the soma is a camera-saturation artifact. Glutamate pipette (schematic drawing) positioned on a basal dendrite; 115 μm from the soma. (B) The actual pixels used for spatial averaging are marked (by different shades of grey) inside each of 6 regions of interest (ROIs). The distances of ROIs from the center of the soma were (in μm): 1 = 100; 2 = 95; 3 = 45; 4 = 75; 5 = 115; and 6 = 165 μm, respectively. (C) Spatially averaged traces are aligned to show the temporal relations between electrical transients in different parts of the dendritic tree. Vertical dashed line marks the timing of the glutamate pulse. (D) The initial fast spikelet (arrow) is present only in dendritic segments distal to the glutamate stimulation site (ROIs 1 and 2). Gaussian low-pass = 90 Hz cutoff.

plateau depolarization (Fig. 1D, ROI 2). In 20 out of 34 neurons tested in this way, the rising phase of the glutamate-evoked dendritic plateau potential was uneventful (asterisk). It would be more correct to say that with the present sensitivity of voltage-sensitive dye measurements, we were not able to detect a fast transient at the beginning of the plateau depolarization. In the remaining 14 neurons, however, the dendritic plateau potential was preceded by a miniature fast spike (spikelet, Fig. 2D, arrows). The inspection of optical signals obtained in neighboring basal dendrites (Fig. 2D, ROIs 4–6) revealed that the initial spikelet was restricted to the target dendrite only. In addition, the most proximal segments of target dendrites showed no signs of the initial peak (ROI 3), thus confirming that this fast electrical transient was a highly localized event, confined only to the distal dendritic segment (ROIs 1 and 2).

In one group of neurons ($n = 8$) we gradually changed the intensity of the glutamate pulse in order
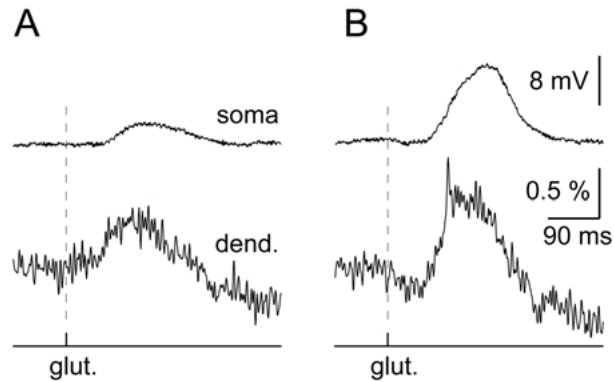
Fig. 3. Glutamate-evoked basal spikelets. (*A*) Recording of the glutamate-evoked membrane potential changes in the cell body (*upper*) and target dendritic segment 85 μm away from the soma (*lower*). Intensity of glutamate iontophoretic current (*I*g) = 0.9 μA. (*B*) Same cell, same camera pixels (spatially averaged), as in the previous panel except that the *I*g = 1.0 μA.

to catch the moment of spikelet initiation. In 5 out of 8 neurons, we surpassed the glutamate threshold for dendritic plateau potential (Milojkovic et al., 2005), but we could not detect the initial spikelet. In the other 3 neurons, the glutamate-evoked dendritic plateau began with a fast spikelet. Interestingly, in 2 neurons, in spite of the initiation of the dendritic spikelet, the somatic signal (whole-cell) remained smooth and uneventful (Fig. 3*B*). That is to say, the rising phase of the membrane charging curve did not carry any apparent sign of the fast spikelet occurring in the basal dendrite. Taken together, these experiments established (1) that glutamatergic excitation can generate fast electrical transients in basal dendrites (spikelets) and (2) the initiation of the dendritic spikelet could easily be missed in somatic recordings.

THE SIGN OF THE DENDRITIC SPIKELET IN SOMATIC RECORDINGS

The majority of neurons in our data set received suprathreshold dendritic stimulation (*n* = 34). As previously stated, 14 out of 34 neurons stimulated in this way exhibited fast dendritic spikelets. In 12 out of 14 spikelet-producing neurons, the onset of the sustained depolarization, recorded by whole-cell pipette, was not smooth, i.e., the rising phase of the signal was interrupted by an event having faster dynamics than the somatic charging curve (inflection). In 8 neurons, this inflection was hardly visible (Fig. 4*C*, arrow), while in 4 cells the somatic charging curve was interrupted by a clear peak (Figs. 5*C*, 6*C*, *arrowheads*). In each of these neurons (*n* = 12) multisite optical recordings revealed the dendritic origin of the electrical transient that coincided with the somatic inflection (Figs. 4–6). The fast electrical transient was most prominent in the dendritic segment at the glutamate injection site (Fig. 2*C* ROI *2*; and
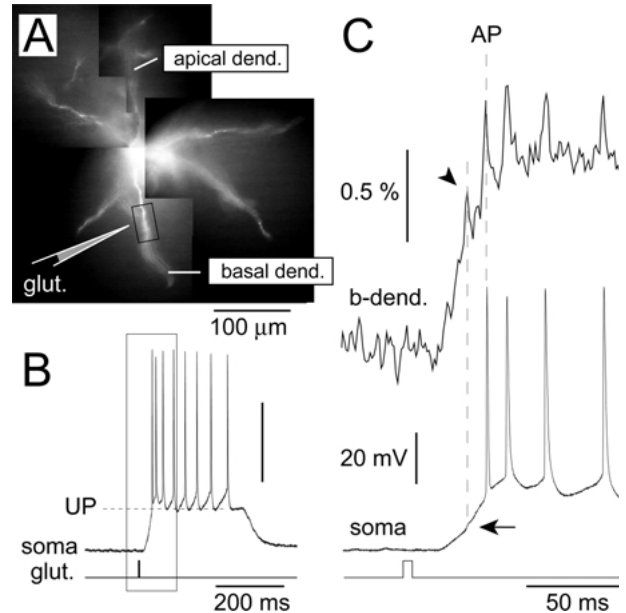

Fig. 4. The signs of basal spikelets in somatic recordings. (*A*) Composite image of JPW1114 filled neuron. The glutamate pipette was positioned 85 μm from the soma. (*B*) Whole-cell recording of glutamate-evoked UP state-like depolarization. Scale = 40 mV. (*C*) The section marked by a rectangle in *B* is aligned with the dendritic optical recording on a faster time scale, to show that the dendritic fast spikelet (*arrowhead*) caused an inflection in the rising phase of the somatic depolarization (*arrow*). The optical signal (*b-dend*) is the product of 18 spatially averaged pixels from the ROI marked by box in *A*. Vertical dashed line (AP) marks the timing of the first somatic action potential.

Fig. 4), or in the dendritic segment distal to the glutamate stimulation site (Fig. 5*B* ROI *1*; and Fig. 6*B* III ROI *1*). The neighboring basal dendrites did not experience fast spikes (Fig. 5, ROIs *7* and *8*). These data established that the ~10 mV spikelet, which precedes plateau depolarization in the somatic whole-cell recording (Figs. 5*C*, 6*C*, *arrowheads*), is a reliable marker of the dendritic fast spike occurring at or near the glutamate stimulation site (*arrows*).

THE SEQUENCE OF EVENTS

Based on the temporal and spatial characterization of membrane potential in the basal dendritic tree (Figs. 1–6), we reconstructed the actual sequence of electrical events in spikelet-producing pyramidal neurons during the suprathreshold glutamatergic excitation. Briefly, a strong glutamate pulse triggers the fast dendritic spikelet that merges into a long-lasting dendritic plateau potential (Fig. 5*B*, ROI *1*). Both the fast spikelet and the plateau potential propagate centripetally towards the cell body, in a decremental fashion (Milojkovic et al., 2004). The low-pass filtering of the dendrite-soma junction severely reduces the amplitude of the fast spikelet, and the spikelet fails to invade the soma (to trigger an
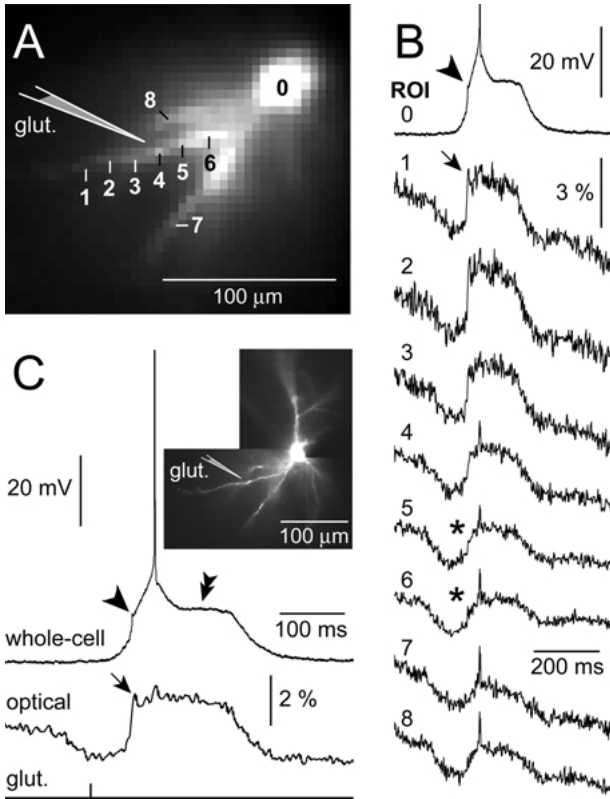
Fig. 5. Fast prepotentials are the hallmark of fast dendritic spikes. (*A*) Image of the JPW1114 filled neuron captured by the fast data acquisition camera. The glutamate stimulation site was on a basal dendrite 80 μm from the soma (schematic drawing). (*B*) Optical signals obtained from three basal dendrites (ROIs *1–8*) are aligned with the somatic whole-cell recording (ROI *0*). Each optical signal is the product of 6 spatially averaged pixel outputs from regions of interest marked by numbers 1–8 in *A*. *Arrowhead*, fast prepotential. *Arrow*, dendritic fast spike. *Asterisk*, uneventful charging curve. (*C*) Pixel outputs from ROIs *1* and *2* were spatially averaged, digitally filtered with a Gaussian low-pass filter (90 Hz cutoff; lower trace), and aligned with the somatic whole-cell record (upper trace) to show the time course and the temporal relationship between the dendritic and somatic signals. *Arrowhead and arrow*, same as in *B*. *Double arrowhead*, plateau phase of the glutamate-evoked depolarization. *Inset*: Composite photograph of the neuron shown in *A*.
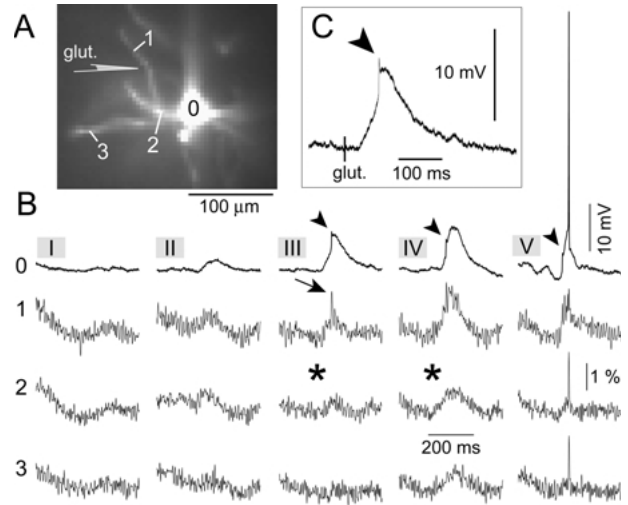

Fig. 6. Initiation of basal spikelets at near threshold glutamate concentrations. (*A*) Fluorescence image obtained with the data acquisition camera. The schematic drawing indicates the position of the glutamate-filled sharp pipette. (*B*) Intensity of glutamate iontophoretic current was gradually increased in five steps (five sweeps *I – V*) from 0.8 to 1.2 μA. Optical signal from the non-target dendrite (ROI *3*) is aligned with optical signals from the target dendrite (ROIs *1 & 2*) and whole cell recording from the soma (ROI *0*), for each stimulus intensity (*I–V*). *Arrowhead*, fast prepotential in somatic recording. *Arrow*, basal spikelet in dendritic optical recording. *Asterisk*, absence of any fast transient. (*C*) The same as in *B* III ROI *0*, shown here on a faster time base.

action potential, Fig. 5*C*, *arrowhead*). With the present sensitivity of our optical measurements, the fast spikelet was not detected in the proximal segment of the target dendrite (Fig. 5*B*, ROIs *5* and *6*; Fig. 6*B*, ROI *2*). Also, in these proximal dendritic segments the onset of the signal was considerably slower (Figs. 5 and 6, *asterisks*) than at the glutamate stimulation site (*arrows*), thus confirming that the fast spikelet does not present itself with the same magnitude and temporal dynamics in all segments of the target basal dendrite (decremental propagation). Although the fast spikelet failed to invade the soma, the long-lasting dendritic plateau potential continues to charge the somatic membrane until the AP threshold is eventually reached (Fig. 5*C*; Fig. 6*B*, V).

The long-lasting somatic depolarization (Fig. 5*C*, *double arrowhead*), also manages to charge the proximal segments of "inactive dendrites" (dendrites that were not exposed to glutamate, Fig. 5*B* ROIs *7* and *8*). In this way, the proximal synaptic contacts in basal dendrites are noticeably depolarized during the glutamate-evoked UP state-like plateau depolarization (backpropagating plateau potential). The long duration of the glutamate-evoked event provides an opportunity for the generation of more than one action potential in the axon-soma trigger zone. All triggered action potentials propagate back in the basal dendritic tree, including the target dendrite (Figs. 1,2, 4, 5, 6, and 7). In approximately 1/3 of the experiments (*n* = 11/34), however, the peaks of the backpropagating APs were not prominent in the segments of target dendrites that were distal to the glutamate stimulation site (Fig. 2*C*, ROI *1*; Fig. 5*B*, ROIs *1–3*; Fig. 6*B*, V, ROI *1*).

SYNAPTICALLY EVOKED DENDRITIC SPIKELETS

So far we determined that exogenous glutamate (glutamate applied iontophoretically) can trigger fast spikelets in basal dendrites. Next, we asked whether basal dendrites can trigger fast spikelets in response to glutamate released from axon terminals (endogenous glutamate). For this purpose, we stimulated basal branches synaptically and monitored membrane
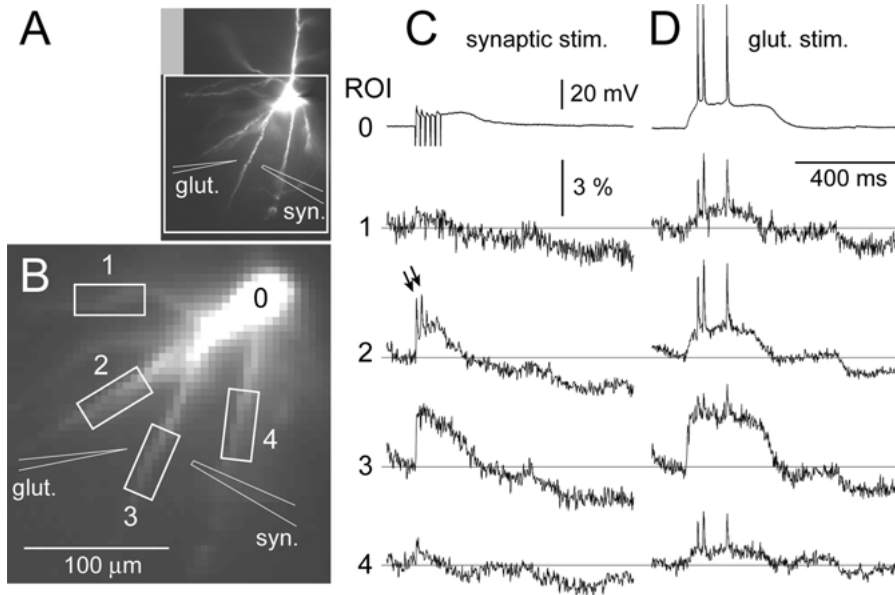
Fig. 7. Synaptically-evoked basal spikelets. (*A*) High resolution fluorescence image of the layer V pyramidal cell. The schematic drawings indicate the positions of glutamate and synaptic stimulation pipettes. (*B*) An area marked with a white rectangle was captured by a fast data acquisition camera (80×80 pixels). (*C*) Recordings of synaptically-evoked membrane potential transients in the cell body (ROI *0*) and basal dendrites, as indicated by boxes in *B*. Stimulus intensity = 30 μA. Duration = 200 μs. Frequency = 50 Hz. Stimulation artifacts have been truncated. Although the synaptic stimulation was intended for dendrite *3*, a substantial synaptic input was received by dendrite *2*; capable of triggering two fast electrical transients (arrows). (*D*) Same cell, same camera pixels as in *C*, except that the neuron was stimulated by glutamate iontophoresis (*I*g = 2.3 μA, duration = 5 ms).

potential changes in the soma (whole-cell) and in the dendrite (optical imaging). In 13 out of 17 neurons, synaptic stimulation produced a clear initial spikelet crowning the beginning of the dendritic plateau potential. In 8 neurons, instead of a single electrical shock, we applied trains of 3–6 pulses (*see* Methods). Quite often (5 out of 8 cells) more than one spikelet was initiated in response to repetitive stimulation. At 50 Hz stimulation frequency, typically 2 initial spikelets were generated in the target dendrite.

The third and later stimuli in the train regularly failed to trigger the fast dendritic transient ($n = 5$, Fig. 7*C*, ROI *2*). Synaptic depression (Thomson, Deuchars & West, 1993; Tsodyks & Markram, 1997), which could have played a role in the dendritic failure to follow 50 Hz stimulation, was not investigated systematically here.

In order to estimate the amplitude of the synaptically-evoked fast spikelet in distal basal dendrites we performed the following experiment. First, we recorded synaptically evoked spikelets (Fig. 7*C*). Then, in the subsequent sweep, we measured the amplitude of the backpropagating AP in the same segment of the same dendrite (Fig. 7*D*). Neurons were kept in the same position and focus between the two consecutive recordings. Having the same dendrite on the same set of camera pixels allowed us to compare signal amplitudes between two consecutive sweeps (*see* Methods). The amplitudes of backpropagating action potentials were noticeably bigger than

the amplitudes of local fast spikelets in dendritic segments 100–150 micrometers from the center of the soma ($n = 4$ neurons, 9 spikelets, 23 backpropagating APs). Comparing each backpropagating AP in the burst with the corresponding spikelet (within the same neuron), yielded the spikelet/AP amplitude ratio of 0.76 ± 0.07 ($n = 23$ comparisons). It should be noted that optical measurements were compromised by poor signal-to-noise ratio (no averaging), and this result should be considered only as a crude estimate of the spikelet-to-BAP amplitude ratio.

In summary, our experimental data indicate that (1) the dendritic spikelet can be evoked in response to synaptic stimulation; (2) at 50 Hz stimulation frequency repetitive pulses can trigger at least 2 spikelets in basal dendrites, (3) under these experimental conditions the triggering process is not robust and failures are common; and (4) the amplitude of the dendritic spikelet is statistically smaller ($p = 0.00016$, $n = 23$) than the amplitude of the backpropagating action potential at distances 100–150 micrometers away from the soma.

INCIDENCE OF THE DENDRITIC SPIKELETS

In the next series of experiments glutamate pulses were delivered to basal dendrites using two different approaches. In the first group of neurons ($n = 42$), fluorescent dyes Rhodamine or Alexa Fluor were injected intracellularly, and glutamate-filled pipettes
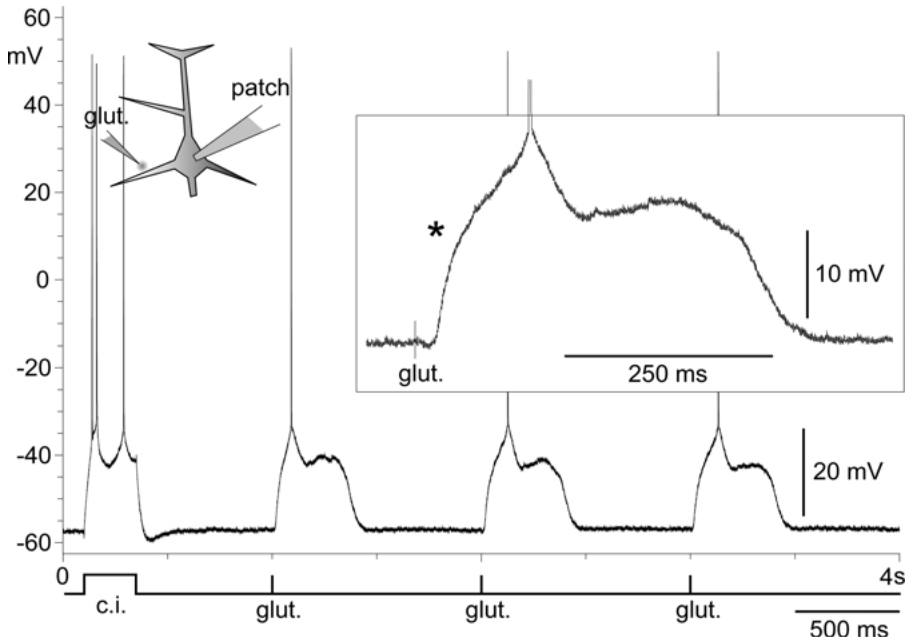
Fig. 8. In the majority of neurons glutamate-evoked plateaus were not accompanied by fast prepotentials. Three glutamate pulses (1 Hz) were applied to a basal dendrite (90 μm from the soma), as indicated in the schematic drawing. The dendritic stimulation site was found using the so called "sniffing for dendrites" technique. To monitor the somatic excitability, three glutamate pulses were preceded by direct current injection (200 pA, 250 ms). *Inset*: The somatic response to a second glutamate pulse is displayed on a faster time base to show the time course of the plateau depolarization. An asterisk marks the initial phase of the somatic signal, where fast prepotentials are expected.

were positioned under visual control, as previously explained for voltage-sensitive dye experiments. In the second group of neurons ($n = 225$) we used the so called "sniffing for dendrites" technique (*see* Methods). In both groups, glutamate pulses (duration = 5 ms, intensity range 0.9–4.2 μA) produced UP-state-like signals, characterized by sustained depolarization (duration > 100 ms, amplitude > 10 mV), having one or more action potentials riding on top (Fig. 8, inset). No difference in the cellular response (sensitivity to glutamate, amplitude and duration of the electrical signal) was detected between the two methodological approaches, and data were pooled together.

A relatively large set of neurons tested in this way ($n = 267$) allowed us to determine the incidence of fast spikelets in somatic recordings. Each neuron in this data set received multiple glutamate pulses; on average 13.44 pulses per cell. In 47 neurons the number of pulses was greater than 20. In 14 neurons the number of glutamate stimulations was greater than 30. In spite of repetitive suprathreshold stimulations, in the majority of pyramidal cells ($n = 220$) we could not detect a single fast spikelet in the somatic whole-cell recording (Fig. 8).

In 47 out of 267 neurons, however, the glutamate-evoked sustained depolarization was preceded by a clearly distinguishable fast spikelet of approximately 10 mV in amplitude (Figs. 9, and 10 inset, *arrowhead*). In 36 spikelet-producing neurons the spikelet initiation was very irregular. Although the tip of the glutamate-filled pipette was kept in a fixed position during the recording sessions, consecutive stimuli produced a large number of failures (Fig. 10, sweeps *1–8*). In this group of pyramidal
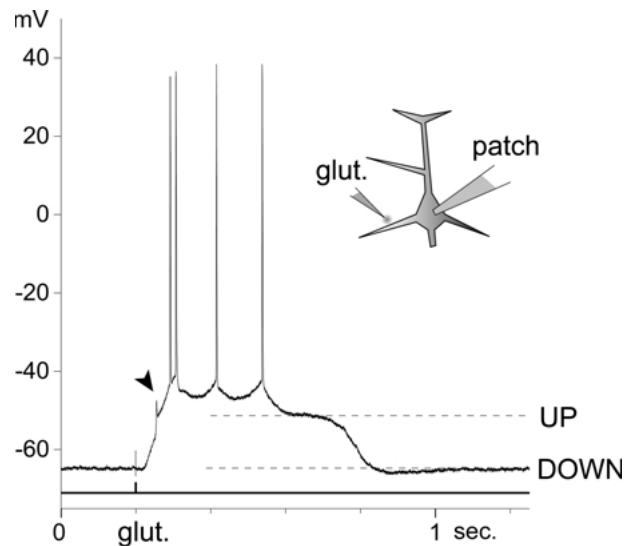

Fig. 9. Fast prepotentials in vitro. A single glutamate pulse was applied to a basal dendrite 95 μm from the soma (Ig, 2.4 μA; duration, 5 ms). One fast spikelet (*arrowhead*) interrupts the charging curve of the UP state-like depolarization.

cells ($n = 36$) spikelets on average occurred in 19.6% of the total number of glutamate stimulations.

In the remaining 11 spikelet-producing neurons the initiation was quite regular (on average 96.7% of the total number of sweeps). In 5 neurons, which exhibited highly regular spikelet firing (~100%), we varied the intensity of the glutamate iontophoretic current in order to determine if the spikelet incidence was dependent on the strength of stimulus (Fig. 11).
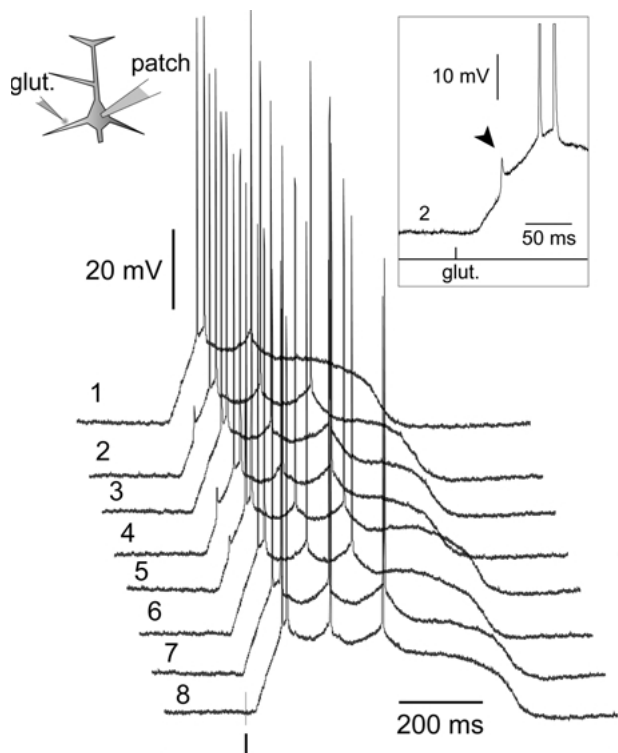
Fig. 10. In the majority of spikelet-producing neurons the spikelet production was unreliable. Glutamate pulses were delivered to the same dendritic segment at an interval of 2–3 seconds. Although the position of the glutamate pipette was kept fixed between trials, fast ~10 mV prepotentials were detected in less than 50% of trials. *Left inset*: Schematic drawing of the experimental paradigm. *Right inset*: A signal from trial *2* is displayed on a faster time base to show the details of the fast spikelet (*arrowhead*). In this and the following figure Arabic numerals indicate the chronological progression of the trials.

The probability of spikelet initiation in these 5 cells was not affected by the stimulus strength, but this is not to say that fast electrical transients were insensitive to glutamate concentration. Careful inspection of the data revealed that in 5 out of 5 cells tested in this way, the gradual increase in glutamate iontophoretic current caused a gradual decline in the peak amplitude of the somatically recorded spikelet (Fig. 11*B*, *C*).

Next, all data obtained in 267 pyramidal cells were pooled together, and the incidence of fast prepotentials in somatic recordings was calculated against the total number of glutamate pulses delivered to the basal dendrites (mean distance from the cell body 74.4 ± 21 μm). Out of 267 neurons tested in this way, only 47 neurons (17.6%) exhibited fast prepotentials in the somatic recordings (Fig. 12*A*). Out of 3589 suprathreshold glutamate pulses delivered on basal dendrites (*see* Methods for definition of "suprathreshold"), only 345 (9.6%) resulted in fast spikelet generation (Fig. 12*B*).

DENDRITIC SPIKELETS ARE TTX-SENSITIVE

In order to investigate whether dendritically-evoked spikelets were mediated by voltage-gated sodium channels we performed experiments illustrated in Fig. 13. Glutamate pulses were applied to basal dendrites, first in normal ACSF (*control*), and then after the bath application of the sodium channel blocker Tetrodotoxin (*TTX*, 1 μM). These experiments were carried out in the group of pyramidal neurons ($n = 5$) that exhibited a highly regular spikelet initiation (Fig. 13, *upper trace*, *arrowheads*). During the entire course of the experiment, the stimulus parameters (location, intensity, duration, and frequency) were kept unchanged. In all spikelet-producing neurons tested in this way ($n = 5$), introduction of TTX abolished both, fast spikelets and somatic action potentials (Fig. 13, *bottom trace*). The sodium-channel antagonist did not affect glutamate-evoked plateau potentials in basal dendrites, as previously reported (Milojkovic et al., 2005). It is worth mentioning that in our laboratory, the effects of TTX on plateau generation were studied in a total of 21 pyramidal cells. Unlike the 5 neurons mentioned above, these 21 cells were characterized with a very low incidence of fast prepotentials (<5%). Nevertheless, with sodium channels fully blocked by TTX (1 μM), all of these cells invariably produced sustained somatic plateau depolarizations in response to suprathreshold glutamatergic excitation (Milojkovic et al., 2005). Not a single glutamate pulse (0 out of 134) was capable of producing the fast initial spikelet in a TTX-treated cell. These two sets of experiments ($n = 5$ and $n = 21$) suggest that fast spikelets, which occasionally precede glutamate-evoked plateau potentials in prefrontal cortex layer V pyramidal neurons (Fig. 9), are mediated by TTX-sensitive voltage-gated sodium channels.

Discussion

Here we present the first conclusive evidence that basal dendrites of cortical pyramidal neurons have the ability to fire local sodium spikes. Local glutamate stimulation was used in earlier studies of basal function (Schiller et al., 2000; Oakley, Schwindt & Crill, 2001b), but fast spikes were not previously detected in basal dendrites of neocortical pyramidal cells. Recently, Ariav et al., (2003) used calcium imaging to determine the origin of fast spikes in CA1 hippocampal neurons. It is well known that the slow component of the synaptically-evoked or glutamate-evoked transient causes strong calcium elevations in thin dendritic branches of neocortical (Schiller et al., 2000) and hippocampal pyramidal neurons (Regehr & Tank, 1990; Wei et al., 2001). Calcium ions stream into the dendritic cytosol through either NMDA
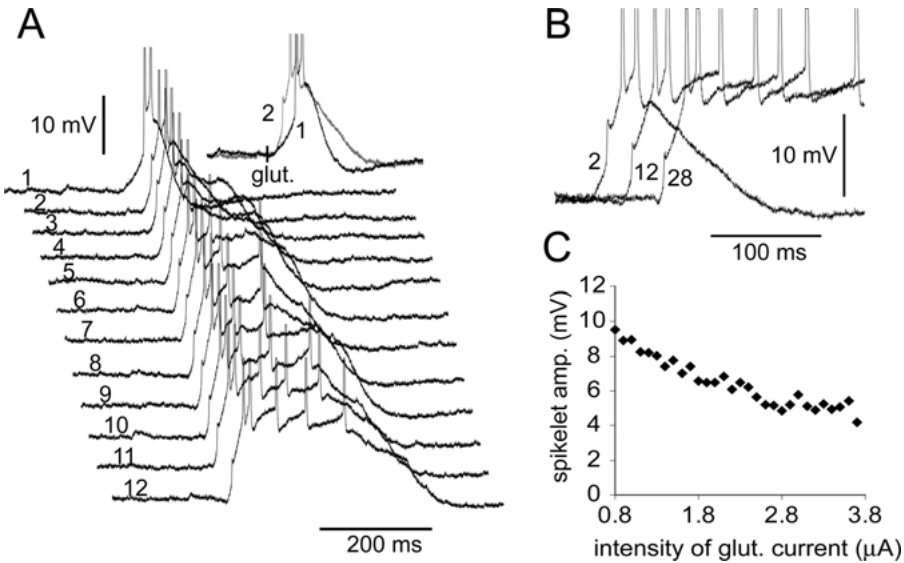
Fig. 11. In some neurons the initiation of dendritic spikelets was very reliable. (*A*) Glutamate pulses of gradually increasing intensity were applied to the same dendritic segment at 2–3 seconds inter-stimulus interval. *Inset*: The fast prepotential was triggered when Ig was increased from 0.8 μA (sweep *1*) to 0.9 μA (sweep *2*). (*B*) Three sweeps are superimposed and shifted in time to show that an increase in glutamate concentration presented to the basal dendrite resulted in a decrease in spikelet amplitude in the soma. Numbers mark the chronological order of the traces. (*C*) The peak amplitude of the basal spikelet in the soma versus the intensity of glutamate iontophoretic current. All glutamate pulses were of equal duration (5 ms). The glutamate pipette was 80 μm from the soma.
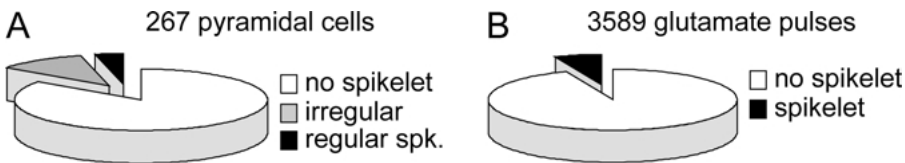

Fig. 12. The overall incidence of fast spikelets is relatively low. (*A*) Of 267 neurons, whose basal dendrites were stimulated with supra-threshold glutamate pulses, only 11 neurons produced fast spikelets in a very regular manner (*black*, ∼100% success rate). 36 neurons produced basal spikelets in a very irregular manner (*grey*, less than 20% of glut. pulses per cell were successful). (*B*) In the data pooled from 267 neurons only 9.6% of the total number of glutamate stimulations (345 out of 3589) produced basal spikelets in somatic recordings.

receptor channels (Schiller et al., 2000), voltage-gated calcium channels (VGCC) (Oakley, Schwindt & Crill, 200la; Wei et al., 2001), or both, NMDA and VGCC (Antic et al., 2003) channels. Because fast spikes were always accompanied by a slow component, the calcium imaging data by Ariav et al., (2003) cannot be used to determine the site of origin, or to describe any other characteristics of fast spikes in the dendrites. In fact, it is still unclear if fast spikelets (alone) produce any calcium transients in basal dendrites. Our multi-site voltage-sensitive dye recordings, on the other hand, unequivocally showed that fast spikelets originated in the basal dendrite, and were not the products of axo-axonal gap junctions (Schmitz et al., 2001).

Besides this direct experimental evidence, our data revealed three novel and important properties of basal spikelets in pyramidal neurons. First, voltage imaging showed that basal spikelets are restricted to only one basal dendrite in the dendritic tree. Second, the actual initiation site (trigger zone) is located at or

distal to the glutamate stimulation site (Figs. 2, 5 and 6). Finally, the amplitude of the dendritically evoked fast spikelet, in dendritic segments 100–150 μm away from the cell body, is always smaller than the amplitude of the backpropagating somatic action potential. These three pieces of information could not have been obtained using somatic whole-cell, or dendritic calcium imaging, or any combination of these two methods.

ARE BASAL SPIKELETS ARTIFACTS OF VOLTAGE-SENSITIVE DYES?

Voltage-sensitive dyes are notorious for the photo-dynamic damage they produce in neuronal plasma membranes (Salzberg et al., 1977). Under some conditions, they are known to cause significant changes in membrane biophysical properties, such as action potential broadening (Antic et al., 1999). Could dye molecules, bound to dendritic plasma membrane,
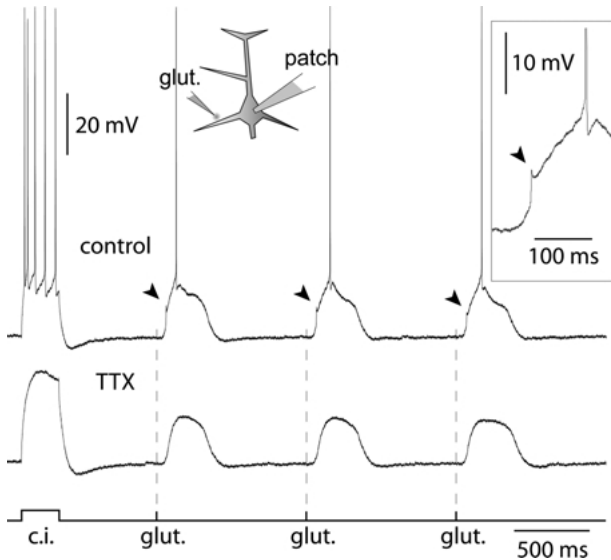
Fig. 13. Fast spikelets are blocked by TTX. Three glutamate pulses (1 Hz) were applied to a basal dendrite, 90 μm from the soma, before (*upper*) and after the introduction of 1 μM TTX into the bath (*lower trace*). All stimulation parameters (location (90 μm), intensity (1.2 μA), duration (5 ms) and frequency (1 Hz)) were kept unchanged; *c.i.* - direct current injection (200 pA, 250 ms). Inset: A characteristic ∼10 mV fast spikelet interrupts the rising phase of the glutamate-evoked plateau depolarization under control conditions (normal ACSF). Arrows mark fast spikelets that follow each glutamate pulse. Vertical dashed lines mark the timing of the glutamate pulses (*glut.*). Note that TTX blocked somatic action potentials and fast prepotentials, but not sustained plateau depolarizations (*lower trace*).

change dendritic excitability and result in a pathological production of fast spikelets? That basal spikelets are not artifacts of voltage-sensitive dye recordings is clear from the fact that fast spikelets were documented in 47 dye-free pyramidal neurons upon glutamatergic stimulation of basal dendrites (Figs. 8–13).

ARE BASAL SPIKELETS ARTIFACTS OF GLUTAMATE IONTOPHORESIS?

Strong current pulses delivered to glutamate-filled glass pipettes can potentially eject a large number of glutamate ions and produce greater concentrations of glutamate at the tip of the pipette than are normally achieved under physiological conditions (Clements, 1996). It is therefore necessary to consider whether, perhaps, the generation of basal spikelets is due to a very high local concentration of iontophoretically ejected glutamate. We answered this question experimentally (Fig. 7C). It is unlikely that basal spikelets are artifacts of glutamate microiontophoresis, because they can be evoked synaptically, by endogenous glutamate release from axon terminals in the brain slice (n = 13 neurons). In addition, intracellular recordings from neocortical pyramidal neurons

have shown that this neuronal type experiences fast spikelets in vivo (Steriade et al., 1993b). Fast prepotentials, approximately 10 mV in amplitude, and having a time course that is an order of magnitude faster than that of an EPSP, were evoked by both thalamic and cortical stimulations in intact animals (Steriade et al., 1993b), their figure 2). Interestingly, Steriade and colleagues (1993 a, b) studied the morphology of pyramidal neurons they recorded from, and found that UP-state- and spikelet-producing neurons were characterized by luxuriant basal dendritic arbors.

THE INCIDENCE OF BASAL SPIKELETS

In some intracellular recordings from neocortical pyramidal neurons in vivo, fast prepotentials are rare or completely absent (Nunez, Amzica & Steriade, 1993; Steriade, Nunez & Amzica, 1993a; Lewis & O'Donnell, 2000; Timofeev et al., 2000). According to our relatively large data set (267 neurons), the incidence of fast spikelets in vitro does not seem to be much higher than that observed in vivo. The great majority of cells in the present study (83%) did not generate a single fast prepotential, in spite of multiple suprathreshold glutamate stimulations (13.4 stimulations per neuron). In 76% of neurons that did produce fast spikelets, this process was highly irregular (only 3% of glutamate pulses were successful). There are three reasons that might account for low incidence of basal spikelets in somatic recordings. First, the density of voltage-gated sodium channels in basal dendrites could be very similar to that found in the apical trunk (Stuart & Sakmann, 1994). This relatively low density of sodium channels gives the dendritic membrane some limited ability to produce fast regenerative potentials, and hence the dendritic excitability was dubbed "weak excitability" (Rapp, Yarom & Segev, 1996; Larkum et al., 1998; Mackenzie & Murphy, 1998; Poznanski, 2002). Experiments with direct or synaptic dendritic stimulation have shown that regenerative sodium potentials can be evoked in the apical trunk, but the intensity of the input needed to be considerably higher that that in the soma-axon region (Stuart & Sakmann, 1994; Golding & Spruston, 1998; Hausser et al., 2000). Thus, the distal dendritic regions of mammalian CNS neurons are not properly equipped to fire full-size sodium action potentials. An exception to this rule is the mitral cell of the olfactory bulb. Dendritic patch and voltage-sensitive dye measurements showed that full-size sodium action potentials are regularly triggered in the apical tuft of the mitral primary dendrites (Chen, Midtgaard & Shepherd, 1997; Djurisic et al., 2004). In the present study the peak amplitude of the fast spikelet in the remote dendritic region was always smaller than the amplitude of the backpropagating AP (Fig. 7C, D).

Backpropagating APs have the advantage of being generated in the soma. They start with impressive amplitudes ($\sim$ 100 mV), and even in the absence of dendritic sodium conductance they can backpropagate passively and cause substantial voltage transients in basal dendrites, as revealed in the detailed multi-compartmental models of the pyramidal layer V neuron (Rapp et al., 1996; Vetter, Roth & Hausser, 2001; Antic, 2003). Locally triggered basal spikelets on the other hand, not only lack the passive boost of the somatic AP, but even worse, their generator current is sucked up by an enormous nearby current sink – the cell body. That a sudden increase in diameter at a neurite-soma junction presents a serious obstacle for propagation of sodium spikes has been shown previously in computer simulations (Goldstein & Rall, 1974; Parnas, Hochstein & Parnas, 1976; Archie & Mel, 2000; Hossain et al., 2005), and, most importantly, in experimental measurements of action potential propagation from the neuronal process into the soma (Tauc, 1962; Ramon, Joyner & Moore, 1975; Golding & Spruston, 1998; Antic et al., 2000; Golding, Staff & Spruston, 2002). Therefore, the relatively low density of sodium channels in basal dendrites, in combination with the proximity of the cell body, might be responsible for the low incidence of basal spikelets in the somatic recordings (Fig. 12).

The third reason why sodium spikelets are so seldom observed in the somatic recordings might be the glutamate shunt. We have shown previously that the plateau phase of the glutamate-evoked dendritic potential is due to the saturation of the membrane response at the stimulation site. Once the plateau has been reached, further increase in glutamate concentration does not contribute to the amplitude of membrane potential change in the target dendrite (Milojkovic et al., 2005). Given the high density of excitatory synaptic contacts (and, accordingly, the high density of ionotropic glutamate receptor-channels) in basal dendrites of pyramidal neurons (Larkman, 1991), especially in prefrontal pyramids (Elston, 2003), the plateau phase of the dendritic potential represents a very high conductance state. A dendritic segment in this state exerts a considerable shunting effect on local fast regenerative transients. Our data showed that sodium spikelets are often triggered in the dendritic regions adjacent to (Fig. 2) or distal to the glutamate stimulation site (Fig. 5). In the latter case, the leaky (high conductance) segment (Fig. 5B, ROI 3) is right between the spikelet initiation site (distal dendrite) and the cell body. Therefore, the plateau-producing dendritic segment may present an obstacle to forward propagation of fast electrical transients to the soma. This is consistent with the mechanism by which the large conductance change underlying the AP is actually shunting EPSPs in proximal dendritic segments (Hausser, Major & Stuart, 2001). In the present example, a fast spikelet,

which is a product of sparse voltage-gated sodium channels, is likely to be eclipsed by large glutamate-evoked dendritic conductance. We showed that basal spikelets are clearly detectable in the distal segment, but very weak in the proximal region of the glutamate-exposed branch (Figs. 5B, and 6B, asterisks). Finally, in neurons characterized by reliable production of fast prepotentials, an increase in glutamate iontophoretic current intensity regularly caused a reduction in the peak amplitude of the fast prepotential (Fig. 11C).

In summary, the high conductance state of the glutamate-exposed dendritic segment, in combination with the dendrite-soma impedance mismatch (and low density of voltage-gated sodium channels), are the three most likely reasons why excitatory glutamatergic stimulations of basal branches rarely produce obvious fast prepotentials in the somatic recordings (Fig. 9).

THE FUNCTIONAL ROLE OF BASAL SPIKELETS

The role of fast spikes in basal dendrites of hippocampal CA1 neurons has been described as markedly improving the temporal precision and stability of output axonal action potentials by contributing large fast voltage transients at the soma (Ariav, Polsky & Schiller, 2003). Two lines of evidence suggest that this role for basal spikes is somewhat exaggerated. First, the fact that, at the resting membrane potential, basal spikes produce fast voltage transients at the soma, and not action potentials (Ariav et al., 2003), clearly shows that these dendritic events are essentially ineffective. Basal spikes in vitro do not have the ability to drive the axonal output on their own (Figs. 9 and 10). Quite the opposite is true for glutamate-evoked dendritic plateau potentials. Dendritic plateau potentials, which originate in the same section of the basal dendrite as fast spikes, provide a very reliable drive for bursts of action potentials (Milojkovic et al., 2004). The second piece of evidence against basal spikes acting as precise temporal encoders consists of in vivo recordings of fast prepotentials. Spontaneous synaptic activity in vivo is much higher than in vitro (Waters & Helmchen, 2004). Even in the preserved synaptic background (in vivo), putative dendritic spikes very often fail to trigger an action potential in neocortical pyramidal neurons. Not even the pairing of spontaneous synaptic activity with artificial soma depolarization could prevent the high failure rate of fast dendritic spikes in triggering somatic action potentials ((Steriade et al., 1993b), their figure 4A).

If basal spikelets are not the ultimate temporal encoders, what is then their role in cortical processing? Depending on the neuronal physiological state the functional significance of basal spikes could be one of the following four:

(1) During the generation of dendritic plateau

potentials fast basal spikelets may serve to link the AMPA-mediated depolarization with the calcium-NMDA plateau potential (spike-chain mechanism (Schiller et al., 2000)). The dendritic plateau potentials were shown to play the critical role in the in vitro model of the cortical pyramidal neuron UP state (Milojkovic et al., 2004; 2005).

(2) In pyramidal cells in the DOWN state, basal spikes may be involved in so-called "action potential-independent synaptic plasticity". Namely, synaptic contacts in distal regions of spikelet-producing dendrites may experience depolarization-dependent long-term potentiation in the absence of somatic action potential firing (Golding et al., 2002).

(3) Isolated fast spikes in basal dendrites may mediate the dendritic release of retrograde messengers (Zilberter, 2000; Trettel, Fortin & Levine, 2004). In this way, the postsynaptic membrane can communicate with its presynaptic counterparts during the synchronous activation of the cluster of excitatory synaptic inputs impinging on one basal dendrite, in situations when the level of excitation is not strong enough to discharge the soma-axon compartment. In both scenarios "2" and "3", the pyramidal cell is not producing an output (action potential) and yet the restricted population of synaptic contacts is modulated according to the Hebbian rule.

(4) Only in strongly depolarized pyramidal neurons the fast basal spikes may serve to improve the temporal precision of the somatic action potential (Softky, 1994; Konig, Engel & Singer, 1996; deCharms & Zador, 2000; Ariav et al., 2003).

On the other hand, it is also conceivable that fast spikes in basal dendrites do not have any functional role in signal integration, whatsoever. Basal spikelets could perhaps be just a side product of sodium channel proteins that were originally placed there to support action potential backpropagation in thin dendrites (Antic, 2003). These and other hypotheses concerning the functional significance of basal spikes, and their potential role in cortical signal processing, are currently under active investigation.

References

Antic, S.D. 2003. Action potentials in basal and oblique dendrites of rat neocortical pyramidal neurons. *J. Physiol.* **550:**35–50

Antic, S., Major, G., Zecevic, D. 1999. Fast optical recordings of membrane potential changes from dendrites of pyramidal neurons. *J. Neurophysiol.* **82:**1615–1621

Antic, S., Wuskell, J.P., Loew, L., Zecevic, D. 2000. Functional profile of the giant metacerebral neuron of Helix aspersa: temporal and spatial dynamics of electrical activity in situ. *J. Physiol.* **1:**55–69

Antic, S., Zecevic, D. 1995. Optical signals from neurons with internally applied voltage-sensitive dyes. *J. Neurosci.* **15:**1392–1405

Antic S.D., Radojicic M.S., Milojkovic B.A., Goldman-Rakic, P.S. 2003. Ionic basis of glutamate evoked spikes in basal dendrites of pyramidal neurons in prefrontal cortex. *Soc. Neurosci. Abstr.*:476.10

Archie, K.A., Mel, B.W. 2000. A model for intradendritic computation of binocular disparity. *Nat. Neurosci.* **3:**54–63

Ariav, G., Polsky, A., Schiller, J. 2003. Submillisecond precision of the input-output transformation function mediated by fast sodium dendritic spikes in basal dendrites of CA1 pyramidal neurons. *J. Neurosci* **23:**7750–7758

Bekkers, J.M. 2000. Distribution and activation of voltage-gated potassium channels in cell-attached and outside-out patches from large layer 5 cortical pyramidal neurons of the rat. *J. Physiol.* **3:**611–620

Chen, W.R., Midtgaard, J., Shepherd, G.M. 1997. Forward and backward propagation of dendritic impulses and their synaptic control in mitral cells. *Science* **278:**463–467

Clements, J.D. 1996. Transmitter timecourse in the synaptic cleft: its role in central synaptic function. *Trends Neurosci.* **19:**163–71

Davila, H.V., Cohen, L.B., Salzberg, B.M., Shrivastav, B.B. 1974. Changes in ANS and TNS fluorescence in giant axons from Loligo. *J. Membrane. Biol.* **15:**29–46

deCharms, R.C., Zador, A. 2000. Neural representation and the cortical code. *Annu. Rev. Neurosci.* **23:**613–647

Djurisic, M., Antic, S., Chen, W.R., Zecevic, D. 2004. Voltage imaging from dendrites of mitral cells: EPSP attenuation and spike trigger zones. *J. Neurosci.* **24:**6703–6714

Elston, G.N. 2003. Cortex, cognition and the cell: New insights into the pyramidal neuron and prefrontal function. *Cereb. Cortex.* **13:**1124–1138

Feldmeyer, D., Lubke, J., Silver, R.A., Sakmann, B. 2002. Synaptic connections between layer 4 spiny neurone-layer 2/3 pyramidal cell pairs in juvenile rat barrel cortex: physiology and anatomy of interlaminar signalling within a cortical column. *J. Physiol.* **538:**803–822

Frick, A., Magee, J., Koester, H.J., Migliore, M., Johnston, D. 2003. Normalization of Ca^{2+} signals by small oblique dendrites of CA1 pyramidal neurons. *J. Neuro sci* **3:**3243–3250

Golding, N.L., Spruston, N. 1998. Dendritic sodium spikes are variable triggers of axonal action potentials in hippocampal CAl pyramidal neurons. *Neuron* **21:**1189–1200

Golding, N.L., Staff, N.P., Spruston, N. 2002. Dendritic spikes as a mechanism for cooperative long-term potentiation. *Nature* **418:**326–331

Goldstein, S.S., Raill, W. 1974. Changes of action potential shape and velocity for changing core conductor geometry. *Biophys. J.* **14:**731–757

Grinvald, A., Salzberg, B.M., Lev-Ram, V., Hildesheim, R. 1987. Optical recording of synaptic potentials from processes of single neurons using intracellular potentiometric dyes. *Biophys. J.* **51:**643–651

Gulledge, A.T., Kampa, B.M., Stuart, G.J. 2005. Synaptic integration in dendritic trees. *J. Neurobiol.* **64:**75–90

Hassner, A., Birnbaum, D., L.M. 1984. Chargeshift probes of membrane potential. Synthesis. J. Org. Chem. **49:**2546–2551

Hausser, M., Major, G., Stuart, G.J. 2001. Differential shunting of EPSPs by action potentials. *Science* **291:**138–141

Hausser, M., Spruston, N., Stuart, G.J. 2000. Diversity and dynamics of dendritic signaling. *Science* **290:**739–744

Hossain, W.A., Antic, S.D., Yang, Y., Rasband, M.N., Merest, D.K. 2005. Where is the spike generator of the cochlear nerve? Voltage-gated sodium channels in the mouse cochlea. *J. Neurosci.* **25:**6857–6868

Konig, P., Engel, A.K., Singer, W. 1996. Integrator or coincidence detector? The role of the cortical neuron revisited. *Trends Neurosci.* **19:**130–137

Larkman, A.U. 1991. Dendritic morphology of pyramidal neurones of the visual cortex of the rat: III. Spine distributions. *J. Comp. Neurol.* **306:**332–343

Larkum, M.E., Launey, T., Dityatev, A., Luscher, H.R. 1998. Integration of excitatory postsynaptic potentials in dendrites of motoneurons of rat spinal cord slice cultures. *J. Neurophysiol.* **80:**924–935

Larkum, M.E., Zhu, J.J., Sakmann, B. 2001. Dendritic mechanisms underlying the coupling of the dendritic with the axonal action potential initiation zone of adult rat layer 5 pyramidal neurons. *J. Physiol.* **533:**447–466

Lewis, B.L., O'Donnell, P. 2000. Ventral tegmental area afferents to the prefrontal cortex maintain membrane potential 'up' states in pyramidal neurons via D(l) dopamine receptors. *Cereb. Cortex* **10:**1168–1175

Loew, L.M., Cohen, L.B., Dix, J., Fluhler, E.N., Montana, V., Salama, G., Wu, J.Y. 1992. A naphthyl analog of the aminostyryl pyridinium class of potentiometric membrane dyes shows consistent sensitivity in a variety of tissue, cell, and model membrane preparations. *J. Membrane Biol.* **130:**1–10

London, M., Hausser, M. 2005. Dendritic computation. *Annu. Rev. Neurosci.* **28:**503–532

Mackenzie, P.J., Murphy, T.H. 1998. High safety factor for action potential conduction along axons but not dendrites of cultured hippocampal and cortical neurons. *J. Neurophysiol.* **80:**2089–2101

Magee, J.C. 2000. Dendritic integration of excitatory synaptic input. *Nat. Rev. Neurosci.* **1:**181–190

Magee, J.C., Johnston, D. 1995. Characterization of single voltage-gated Na^+ and Ca^{2+} channels in apical dendrites of rat CA1 pyramidal neurons. *J. Physiol.* **487:**67–90

Migliore, M., Shepherd, G.M. 2002. Emerging rules for the distributions of active dendritic conductances. *Nat. Rev. Neurosci.* **3:**362–370

Milojkovic, B.A., Radojicic, M.S., Antic, S.D. 2005. A strict correlation between dendritic and somatic plateau depolarizations in the rat prefrontal cortex pyramidal neurons. *J. Neurosci.* **25:**3940–3951

Milojkovic, B.A., Radojicic, M.S., Goldman-Rakic, P.S., Antic, S.D. 2004. Burst generation in rat pyramidal neurones by regenerative potentials elicited in a restricted part of the basilar dendritic tree. *J. Physiol.* **558:**193–211

Nunez, A., Amzica, F., Steriade, M. 1993. Electrophysiology of cat association cortical cells in vivo: intrinsic properties and synaptic responses. *J. Neurophysiol.* **70:**418–430

Oakley, J.C., Schwindt, P.C., Grill, W.E. 2001a. Dendritic calcium spikes in layer 5 pyramidal neurons amplify and limit transmission of ligand-gated dendritic current to soma. *J. Neurophysiol.* **86:**514–527

Oakley, J.C., Schwindt, P.C., Grill, W.E. 2001b. Initiation and propagation of regenerative Ca^{2+} dependent potentials in dendrites of layer 5 pyramidal neurons. *J. Neurophysiol.* **86:**503–513

Parnas, I., Hochstein, S., Parnas, H. 1976. Theoretical analysis of parameters leading to frequency modulation along an inhomogeneous axon. *J. Neurophysiol.* **39:**909–923

Poirazi, P., Brannon, T., Mel, B.W. 2003. Pyramidal neuron as two-layer neural network. *Neuron* **37:**989–999

Poznanski, R.R. 2002. Dendritic integration in a recurrent network. *J. Integr. Neurosci.* **1:**69–99

Ramon, F., Joyner, R.W., Moore, J.W. 1975. Propagation of action potentials in inhomogeneous axon regions. *Fed. Proc.* **34:**1357–1363

Rapp, M., Yarom, Y., Segev, I. 1996. Modeling back propagating action potential in weakly excitable dendrites of neocortical pyramidal cells. *Proc. Natl. Acad. Sci. USA* **93:**11985–11990

Regehr, W.G., Tank, D.W. 1990. Postsynaptic NMDA receptor-mediated calcium accumulation in hippocampal CA1 pyramidal cell dendrites. *Nature* **345:**807–810

Salzberg, B.M., Grinvald, A., Cohen, L.B., Davila, H.V., Ross, W.N. 1977. Optical recording of neuronal activity in an invertebrate central nervous system: simultaneous monitoring of several neurons. *J. Neurophysiol.* **40:**1281–1291

Schiller, J., Major, G., Koester, H.J., Schiller, Y. 2000. NMDA spikes in basal dendrites of cortical pyramidal neurons. *Nature* **404:**285–289

Schmitz, D., Schuchmann, S., Fisahn, A., Draguhn, A., Buhl, E.H., Petrasch-Parwez, E., Dermietzel, R., Heinemann, U., Traub, R.D. 2001. Axo-axonal coupling, a novel mechanism for ultrafast neuronal communication. *Neuron* **31:**831–840

Shepherd G.M. 2004. The synaptic organization of the brain. Oxford Univ. Press, New York

Shipp, S., Zeki, S. 2002. The functional organization of area V2, I: specialization across stripes and layers. *Vis. Neurosci.* **19:**187–210

Softky, W. 1994. Sub-millisecond coincidence detection in active dendritic trees. *Neuroscience* **58:**13–41

Spruston, N., Schiller, Y., Stuart, G., Sakmann, B. 1995. Activity-dependent action potential invasion and calcium influx into hippocampal CA1 dendrites. *Science* **268:**297–300

Steriade, M., Nunez, A., Amzica, F. 1993a. Intracellular analysis of relations between the slow (< 1 Hz) neocortical oscillation and other sleep rhythms of the electroencephalogram. *J. Neurosci.* **13:**3266–3283

Steriade, M., Nunez, A., Amzica, F. 1993b. A novel slow (< 1 Hz) oscillation of neocortical neurons in vivo: depolarizing and hyperpolarizing components. *J. Neurosci.* **13:**3252–3265

Stuart, G., Schiller, J., Sakmann, B. 1997. Action potential initiation and propagation in rat neocortical pyramidal neurons. *J. Physiol.* **505:**617–632

Stuart, G., Spruston, N. 1998. Determinants of voltage attenuation in neocortical pyramidal neuron dendrites. *J. Neurosci.* **18:**3501–3510

Stuart, G., Sakmann, B. 1994. Active propagation of somatic action potentials into neocortical pyramidal cell dendrites. *Nature* **367:**69–72

Tauc, L. 1962. Site of origin and propagation in spike in the giant neuron of Aplysia. *J. Gen. Physiol.* **45:**1077–1097

Thomson, A.M., Deuchars, L, West, D.C. 1993. Large, deep layer pyramid-pyramid single axon EPSPs in slices of rat motor cortex display paired pulse and frequency-dependent depression, mediated presynaptically and self- facilitation, mediated postsynaptically. *J. Neurophysiol.* **70:**2354–2369

Timofeev, I., Grenier, F., Bazhenov, M., Sejnowski, T.J., Steriade, M. 2000. Origin of slow cortical oscillations in deafferented cortical slabs. *Cereb. Cortex* **10:**1185–1199

Trettel, J., Fortin, D.A., Levine, E.S. 2004. Endocannabinoid signalling selectively targets perisomatic inhibitory inputs to pyramidal neurones in juvenile mouse neocortex. *J. Physiol.* **556:**95–107

Trimmer, J.S., Rhodes, K.J. 2004. Localization of voltage-gated ion channels in mammalian brain. *Annu. Rev. Physiol.* **66:**477–519

Tsodyks, M.V., Markram, H. 1997. The neural code between neocortical pyramidal neurons depends on neurotransmitter release probability. *Proc. Natl. Acad. Sci. USA* **94:**719–723

Vetter, P., Roth, A., Hausser, M. 2001. Propagation of action potentials in dendrites depends on dendritic morphology. *J. Neurophysiol.* **85:**926–937

Waters, J., Helmchen, F. 2004. Boosting of action potential backpropagation by neocortical network activity in vivo. *J. Neurosci.* **24:**11127–11136

Wei, D.S., Mei, Y.A., Bagal, A., Kao, J.P., Thompson, S.M., Tang, C.M. 2001. Compartmentalized and binary behavior of terminal dendrites in hippocampal pyramidal neurons. *Science* **293:**2272–2275

Zilberter, Y. 2000. Dendritic release of glutamate suppresses synaptic inhibition of pyramidal neurons in rat neocortex. *J. Physiol.* **528:**489–496